Effect of Bend Curvature Ratio on Flow Pattern at a Mixing Tee after a 90 Degree Bend

Mohammadreza Nematollahi   nema@shirazu.ac.ir
School of Mechanical Engineering
Shiraz University
Shiraz, 71348-51154, Iran

Mohammad Nazififard   mnazifi@shirazu.ac.ir
School of Mechanical Engineering
Shiraz University
Shiraz, 71348-51154, Iran

Maziar Asmani   maziarasmani@yahoo.com
School of Electrical and Computer Engineering
Iran Azad University of Qeshm Branch
Qeshm Free Area, 795151393, Iran

Hidetoshi Hashizume   hidetoshi.hashizume@qse.tohoku.ac.jp
School of Engineering/Department of Quantum
Science and Energy Engineering
Tohoku University
Tohoku, 980-8579, Japan

Abstract

Many nuclear power plants report high cycle thermal fatigue in their cooling system, caused by temperature fluctuation in a non-isothermal mixing area. One of these areas is the T-junction, in which fluids of various temperatures and velocities blend. The objective of this research is to classify turbulent jet mechanics in order to examine the flow-field structure under various operating conditions. Furthermore, this research discovers the optimum operating conditions of the mixing tee in this piping system. An experimental model, including the T-junction with a 90 degree bend upstream, is operated to analyze this mixing phenomenon based on the real operation design of the Phenix Reactor. The temperature and velocity data show that a 90 degree bend has a strong effect on the fluid mixing mechanism and the momentum ratio between the main velocity and the branch velocity of the T-junction, which could be an important parameter for the classification of the fluid mixing mechanism. By comparing their mean velocity distributions, velocity fluctuations and time-series data, the behavior of the branch jet is categorized into four types of turbulent jets; sorted from the highest to the lowest momentum ratios, the jets are categorized as follows: the wall jet, the re-attached jet, the turn jet, and the impinging jet. Ultimately, the momentum ration of the turn jet was selected as the optimum

operating condition as it has the lowest velocity and the lowest temperature fluctuations near the wall of the mixing tee.

Keywords: T-Junction, Mixing Phenomena, Secondary Flow, Phenix reactor.

1. INTRODUCTION

Thermal stress arising from temperature fluctuations in the cooling system of nuclear power plants is inevitable. When thermal stress is generated by a sudden change in temperature, the process is referred to as thermal shock; failure under repetitive application of thermal stress has been termed thermal fatigue. The severity of the failure is dependent on the shape of the component, the fluid mixing mechanism, and the temperature distribution and it's fluctuations. Studies of thermal fatigue in power plants were initially carried out for liquid-metal-cooled fast breeder reactors because of the high thermal conductivity of liquid-metal coolants. After many recent thermal fatigue events occurred in various nuclear power plants, such as the French PWR CIVAX in 1998, the Japanese PWR Tsuruga-2 in 1999, the Japanese PWR Tomari-2 in 2003, the focus of thermal striping studies shifted to not only fast breeder reactors, but also light water reactors. The T-junction was selected because it is a component common to the cooling systems of most nuclear power plants, having a high capability of thermal fatigue. Several types of numerical and experimental research have been performed based on the fluid mixing phenomena in the T-junction, such as the evaluation of thermal fatigue [1], the numerical simulation of the mixing phenomenon [2], and the analysis of the flow-field structure [3], all of which considered the T-junction as a single component. Although the T-junction has typically been considered a single component, the mixing tee is usually connected to another part of the complex piping system one of which is a 90 degree bend that typically exists upstream of the T-junction and has strong effects on the mixing mechanism [4,5]. The Particle Image Velocimetry (PIV) technique was used to experimentally investigate the fluid mixing phenomenon in the T-junction area with the 90 degree bend upstream [6–8]. This visualization displays origins of the velocity fluctuations in the T-junction area. The thermo-hydraulic characteristics of the turbulent jet are analyzed to better classify the fluid mixing mechanism. This classification is an important factor in order to categorize operating conditions and estimate the effects of thermal fatigue in each mixing condition in the piping system. The effects of velocity and pipe diameter on the fluid mixing mechanism were investigated to explain the behavior of turbulent jets and different operating conditions. Regarding the reported effects on the fluid mixing mechanism of a 90 degree smooth bend with a carving ratio of 1.41, in the present study attempts have been made to investigate the effects of the bend curvature ratio and the axial distance between the bend and T-junction as the target to find their effects. The results are presented here under the title of "Classification of Turbulent Jet in a T-junction area with a 90 degree Sharp Bend on its Upstream."
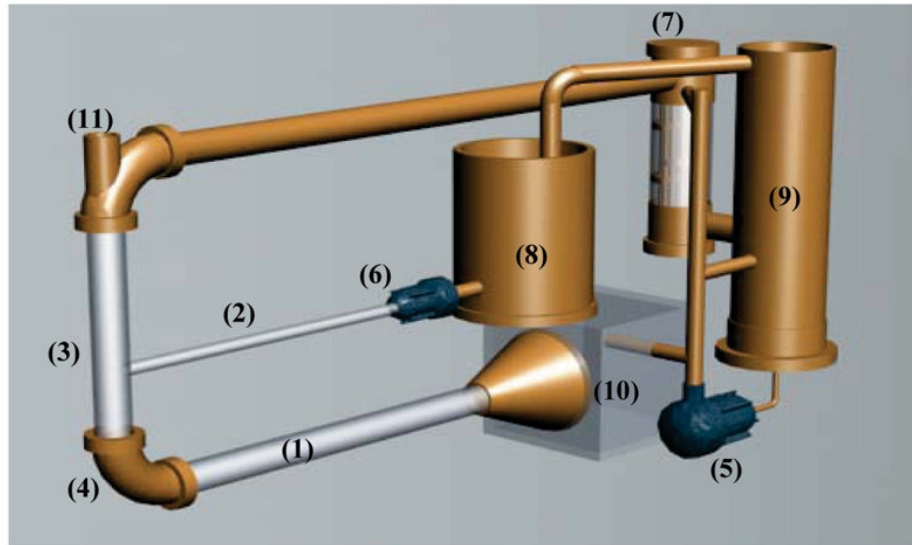
2. PRELIMINARIES

2.1. Experimental apparatuses

The fluid cycle system and T-junction area are shown in Fig. 1. Both the main and branch pipes are made of 3mm thick acrylic circular pipes, and the branch pipe is connected to the main pipe at the right angle to form the mixing tee with a square-edge. The internal main pipe diameter, D_m, is 108 mm and the branch pipe can have one diameter, as well, $D_b = 21$ mm. The main pipe runs vertically upward in the test section, which is connected to a measuring window downstream for visualizing the lateral flow-field.

A 90 degree sharp bend with a carving ratio of one is installed upstream of the T-junction. This bend is stainless steel with a 1.0 curvature ratio. The main flow is straightened by a reducer, a long main pipe before the 90 degree bend ($13D_m$), and a straightener tank made from acrylic

plates with 30 X 30 X 30 cm. The branch pipe is also long enough (60 D_b) to inject fully developed flow into the mixing area.

A heat-exchanger and a heating tank are used to control the inlet temperature of both the main flow and the branch flow in the mixing tee. They are respectively set behind the mixing tank and the branch pump. The heat exchanger has a secondary cooling system for decreasing the temperature with city water. While its flow rate is controlled by an inlet heat-exchanger valve, Whereas the heating tank uses gas and electric heaters to warm the branch flow.

(1) Main Pipe   (2) Branch Pipe   (3) Tee Junction   (4) 90-Degree Bend
(5) Main Pump   (6) Branch Pump   (7) Heat Exchanger (8) Heating Tank
(9) Mixing Tank (10) Straightener Tank (11) Measuring Window

Figure 1. Experimental apparatuses.

The mixing tank is positioned in order to insert small tracers and remove bubbles from the main cycle. This tank is linked to other apparatuses by five pipe connections (the heat-exchanger pipe, emergency inlet pipe, heating tank pipe, main pump pipe and draying outlet pipe). There are two main and branch pumps with 600 and 75 L/min maximum flow rates. A flow rate control valve and an inverter individually adjust the mean velocity of these flows. There is a cube water jacket around the T-junction area which is made of the same acrylic plates as the piping material to decrease the effect of the laser light's refraction through the circular pipe wall during the visualization of the longitudinal sections.

2.2. Experimental conditions and analysis methods

Water was the only working fluid in the experimental loop throughout this research. The PIV system is used to visualize the flow characteristics in the T-junction area. Two conditions are selected to visualize the flow-field, the whole flow-field (long-shot) and the close-up flow-field with 150 mm*150 mm and 60 mm*60 mm view sections, respectively. The resolution of each section is 1018*1008 pixels. The interrogation cell is divided into 64 * 64 pixels at each segment for measuring the whole flow-field and 32 * 32 pixels for measuring a close-up area with a 50% area overlap and 100 time interval. The cross-section is visualized into the radial and axial velocity matrixes ($u_{r,i}$ and $u_{z,i}$). Both matrixes have 30 * 29 arrays when 64 * 64 pixels are cross-correlated, and have 62 * 59 arrays when 32 * 32 pixels cross-correlations are used. The laser sheet thickness is 1–3 mm, with a 200 mJ energy level; this width is selected based on three parameters, the visualization area, the amount of tracer in the fluid and the distance between the visualization cross-section and the camera lens. Two kinds of tracers with different diameters are

used, both made from nylon powder with 1.03 g/cm^3 density. The tracer with an 80 μm diameter is used for visualizing the whole flow-field and a 20 μm diameter for the close-up flow-field condition. The camera starts shooting with a 30 Hz frequency, which has a frame rate of 30 fps in triggered double exposure mode; each shot continually captures 99 images. Forty-nine velocity vector maps are obtained with only 0.03 s time gaps. Five shots are taken, and in total, 240 frames are used to evaluate both flow-fields. The average flow-field and intensity of velocity fluctuation is evaluated by the following equations:

$$U_{ave} = \frac{1}{n}\sum_i^n \sqrt{(u_{r,i}^2 + u_{z,i}^2)} \qquad (1)$$

$$s_j = \left(\frac{1}{n}\sum_{i=1}^n (u_{j,i}-\overline{u}_j)^2\right)^{1/2} \qquad (2)$$

$$U_{mix} = \sqrt{(U_b^2 + U_m^2} \qquad (3)$$

$$I = \sqrt{(s_r + s_z)/2}/U \qquad (4)$$

Where $u_{r,i}$ and $u_{z,i}$ represent the instantaneous radial and axial velocities at the i frame, U_{ave} is the averaged absolute velocity, and n is the total number of the frames. U_b and U_m represent both the branch and main velocities. s_r and s_z are standard deviations of the velocity variation in the radial and axial directions. Lastly, the intensity of the velocity fluctuation represented. Here, both the main and branch flows are entirely in the turbulent regime. The temperature fluctuation intensity, ΔT_{rms}, is calculated at each measuring point from the time-series temperature data and is normalized by using the following equations:

$$\Delta T = T_{branch} - T_{main} \qquad (5)$$

$$\Delta T_{rms} = \left(\sqrt{\sum (Ti - Tm)^2/m}\right)/\Delta T \qquad (6)$$

Where T_i and T_m represent instantaneous temperature and mean temperature, ΔT is the temperature difference between two fluids, and m is total sampling number of the temperature data. Another interesting parameter is fluctuation, which is introduced by: $\sqrt{(u_x - u_{x-1})^2 + (u_y - u_{y-1})^2}$. This parameters show the intensity secondary flow for each position.

3. Results & Discussion

3.1. Classification of turbulent jets

Turbulent jets in finite space show various behaviors. One of these finite spaces is the T-junction area in which two pipes with different diameters and flow are connected together at the right angle with a square-edge. Based on the velocity and momentum ratio of these pipes, the flow pattern in the mixing tee area has different mechanisms, thus many turbulent jets exist. The other parameters used to categorize the mixing mechanism are the Reynolds number of the branch pipe and the Dean number of the main pipe, which are more complicated than the momentum ratio, therefore, they do not show a clear classification of the jets.

Depending on the momentum/velocity ratio of the entering flows from branch pipe and the main pipe, the turbulent mixing patterns can be further divided into four branch jets such as the wall jet, re-attached jet, turn jet and impinging jet. The types of mixing flow are categorized by using the momentum ratio equation as follows:

$$M_R = \frac{\rho_m U_m^2.(D_m \times D_b)}{\rho_b U_b^2.\pi.(D_b/2)^2} \qquad (7)$$

M_R is the momentum ratio, ρ_m and ρ_b are the fluid densities for the main flow and branch flow, U_m and U_b are the mean velocity of the main and branch flow, D_m and D_b are the main and branch pipe diameters.

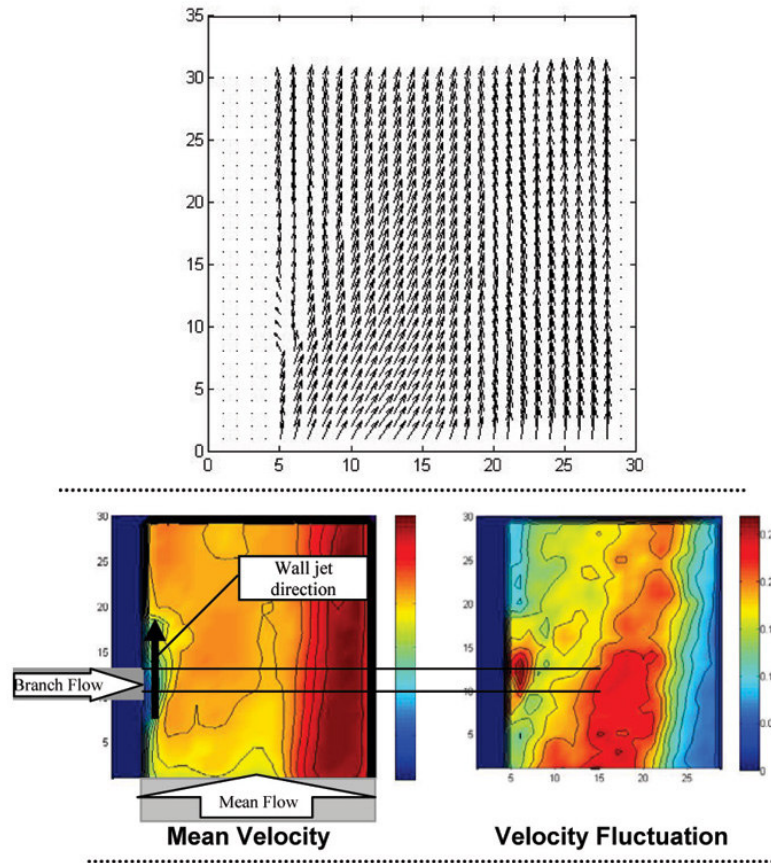**Fig. 2.** Wall jet (Dm = 108 mm, Db = 21 mm, Um = 0.9 m/s, Ub = 0.3 m/s).

For distinguishing these four jets in the flow pattern, we need a basic introduction of each jet and some parameters to distinguish each group. Three parameters are used to investigate their structures and mechanisms: mean velocity distribution, velocity fluctuation and time-series data (Fig. 2).

Attending to these parameters, the branch jets are separated by mean velocity distribution and velocity fluctuation. The mean velocity distribution contains information about the average structure of the jet, while, the velocity fluctuations display the area with the highest variation. In the next step, the time-series data of each condition are investigated to explain the gradual change of the temporal flow structure.

For each condition, 240 frames are used to evaluate the mixing flow mechanism; the first three frames from each condition are shown in Fig.2. Finally, two jets are classified into the aforementioned categories based on the shape and behavior of the branch jets. For providing an exact investigation method for these jets, the structure and mechanism of each jet are described separately:
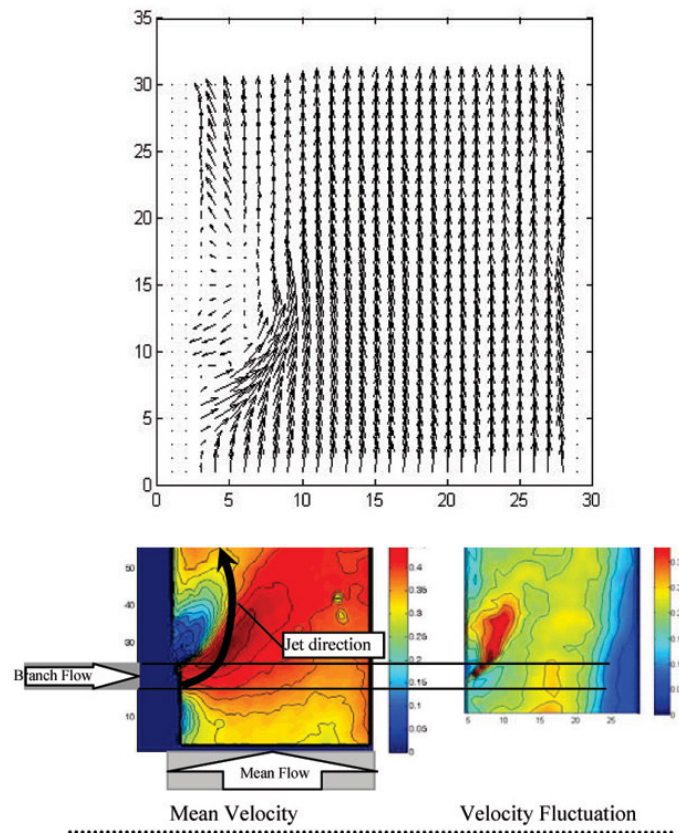
Fig. 3. Wall jet (Dm = 108 mm, Db = 21 mm, Um = 0.6 m/s, Ub = 0.2 m/s).

(a) WALL JET: The wall jet is characterized by a higher main flow and a lower branch flow. Here, the jet does not separate from the main pipe wall. Velocity fluctuations occur only near the wall of the main pipe as shown in Fig. 2.

(b) RE-ATTACHED JET: The re-attached jet is distinguished by an interaction between the secondary flow of the main pipe and the branch flow. The branch jet turns to the center axis of the main pipe and then turns again to the main pipe wall above the branch nozzle in Fig. 3.

(c) TURN JET: The turn jet exists when two inlet flows have comparable momentums, and the branch jet turns to the center axis of the main pipe in the same direction as the main flow provided in Fig. 4.

d) IMPINGING JET: The impinging jet occurs when the branch velocity is much higher than the main velocity, and as a result, the branch flow can touch the opposite wall of the main pipe as visualized in Fig. 5. According to the momentum/velocity ratios between the branch and the main flow, three branch pipe diameters were used to categorize branch jets. In order to categorize flow patterns, 205 conditions were selected.

Each condition was visualized at least five times (240 frames) with the same experimental conditions, such as temperature (18 ºC), 90 degree bend curvature ratio (C_R = 1.0), distance between the 90 degree bend and the branch pipe (d/D_m = 2), etc. By calculating the momentum ratios (M_R) of the main flow and the branch flow based on Eq. (7), a threshold for each flow pattern was defined, as shown in Table 1. Due to many large eddies in the T-junction area with high-mixing Reynolds numbers (Re = 33,000–150,000), it is clear that mainly the mixing phenomena are primarily controlled by the mechanism of these large eddies.

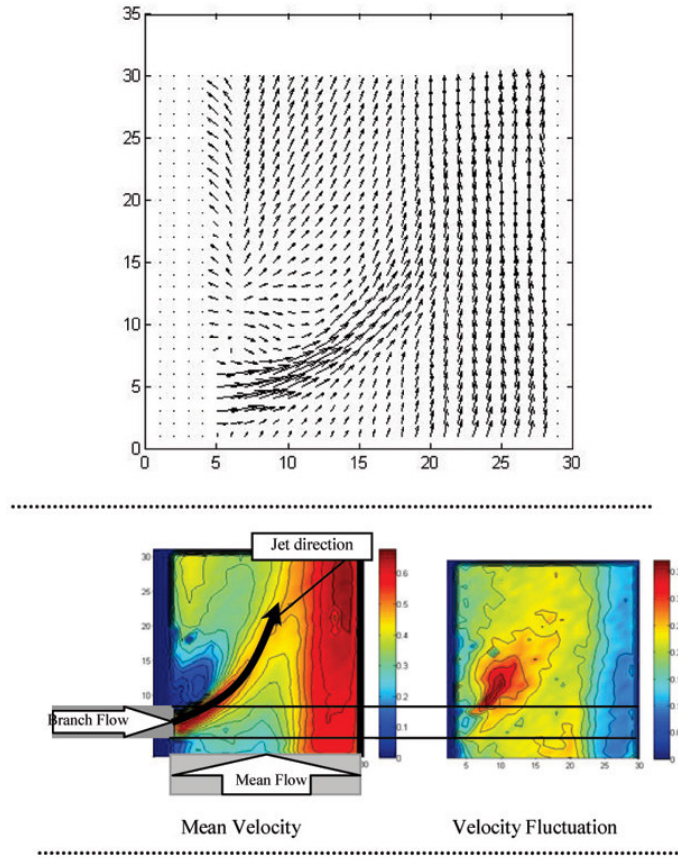**Fig. 4.** Turn jet (D_m = 108 mm, D_b = 21 mm, U_m = 0.6 m/s, U_b = 0.6 m/s).

Table 1. Categorization of the branch jet in T-junction with sharp bend on its upstream

WALL JET	$58 < M_R$
Re-attached jet	$9 < M_R < 38$
Turn jet	$2 < M_R < 9$
Impinging jet	$M_R < 1.5$

3.2. Operating conditions

3.2.1. Momentum ratio effects

Most of these eddies are formed by pipe geometries and an interaction between the main and branch flows [4,6,9]. Fig. 6 shows the maximum intensity of the velocity fluctuation near the wall of the main pipe in the various momentum ratios.

Velocity fluctuation has minimum intensity when the momentum ratio is around M_R = 2.0. Only two main parameters, velocity ratio and branch pipe diameter, can change the momentum ratio. These two parameters provide different mechanisms for the mixing phenomena, and the effects of the velocity ratio and branch pipe diameter are evaluated to consider each mechanism separately. Fig. 7 shows velocity ratio effects on the fluctuation in the 21 mm branch pipe diameters which all categorized with regard to their type of jets. As can be seen in this figure the Phenix reactor Tee junction is located in the re-attached region with a bend by a curving ratio of 1.0.
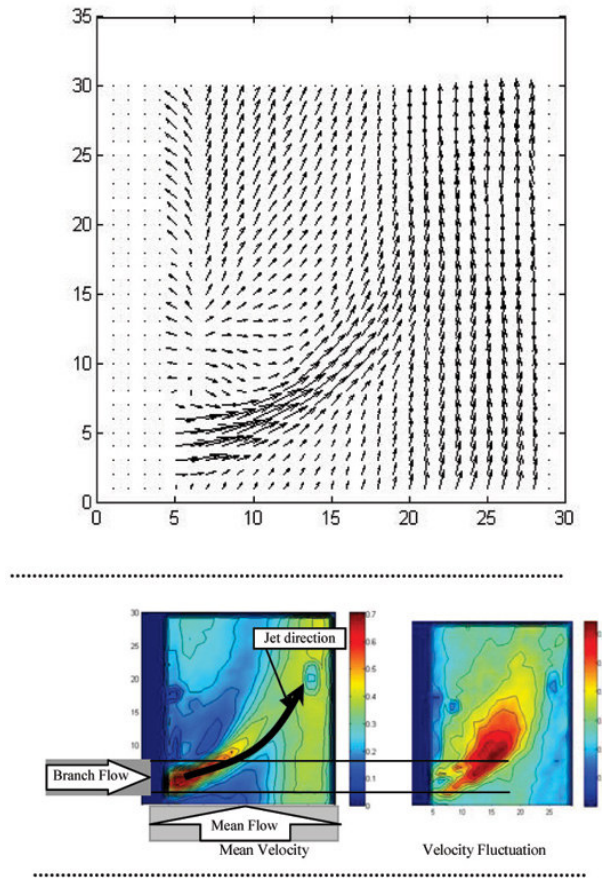
Fig. 5. Impinging jet (Dm = 108 mm, Db = 21 mm, Um = 0.3 m/s, Ub = 0.9 m/s).
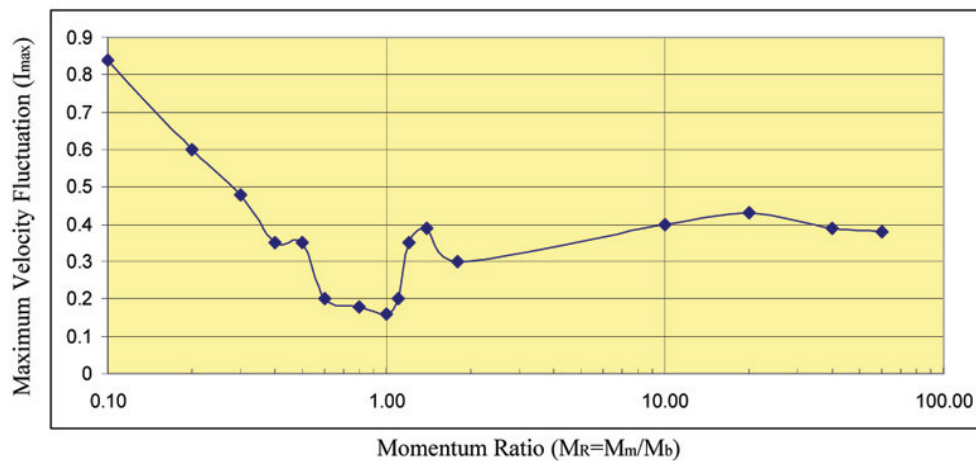

Fig. 6. Maximum intensity of the velocity fluctuation for curving ratio 1.41.

The result shows that for this configuration, by reducing M_R lower than 9, the jet type re-attached reform to the turn jet type. As it is known from equation (7), by reducing the velocity of the main pipe or increasing the velocity of the branch pipe, the lower value of M_R could be achieved. By

changing the bending ratio from 1.41 to 1.0 the results show that most of the data are in the turn jet region. Therefore with the sharpened bend, the re-attached region is compressed.

Since the experimental model is derived from the Phenix reactor structure design, the operating condition of Phenix is compared with other experimental conditions. It is clear that by decreasing the momentum ratio in the T-junction area of the Phenix reactor, the velocity fluctuation decreases. Two parameters have additional effects on the momentum ratio, the aforementioned pipe diameter and velocity.

The momentum is dependent on the diameter, as the following equations show:

$$M_b = C.\frac{1}{D_b^2} \qquad (8)$$

$$C = \frac{4Q_b^2}{\rho_b.\pi} \quad \& \ \ Q_m \text{ and } Q_b = const. \qquad (9)$$

Q_m and Q_b are the constant flow rates in the main and branch pipes, respectively, and ρ_b is the branch flow density. It is important to know that decreasing the branch pipe diameter is helpful until the jet transfers to the optimum condition area. After that, the pipe diameter should no longer change.
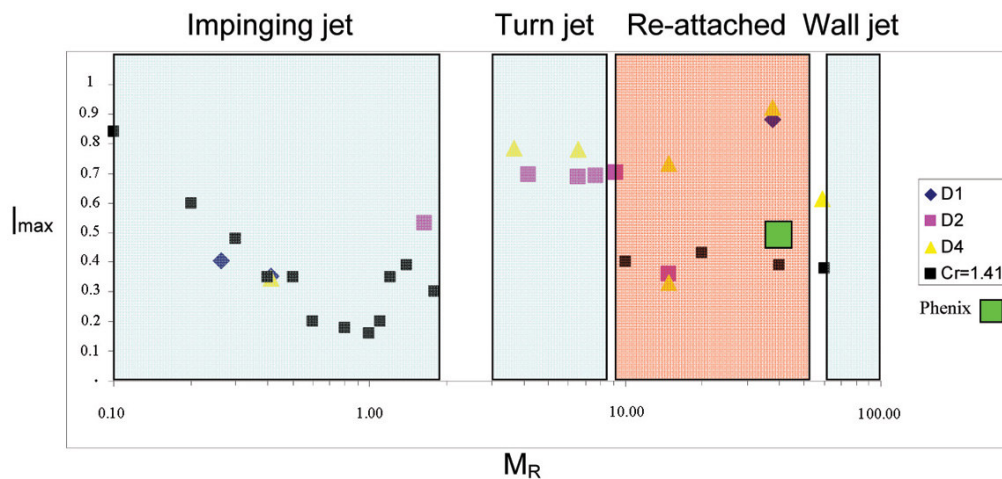

Fig. 7 shows velocity ratio effects on the fluctuation

3.3. Conclusion

The branch jet in the T-junction area acts as a turbulent jet in finite space. Various types of jets exist, dependent on the pipe's geometries and the physical properties of the working fluid. Momentum ratios between the main flow and the branch flow were selected to categorize different groups of branch jets based on the mechanisms and structures of each group. Finally, four groups of turbulent jets with different operating conditions in the T-junction area were introduced, such as the wall jet, re-attached jet, turn jet and impinging jet. The main results of the fluid mixing phenomena are listed as follows:

- By changing the bending ratio from 1.41 to 1.0 the results show that most of data are in the turn jet region. Therefore, with the sharpened bend, the re-attached region is compressed.
- The momentum ratios of the turn jet have the lowest velocity fluctuation.

- The flow rate of the turn jet gradually transfers to the flow rate of the re-attached jet with higher velocity fluctuations by increasing the momentum ratio.
- The flow rate of the turn jet sharply transfers to the flow rate of the impinging jet with a much higher velocity fluctuation, by decreasing the momentum ratio.
- The velocity and temperature fluctuations near the wall decrease by increasing the velocity ratio with a constant flow rate.
- By connecting the branch pipe closer to the bend, the optimum operating conditions transfers to the lower momentum ratio and becomes wider.
- The secondary flow of bend has strong effects on the fluid mixing in the T-junction and pushes the jet into a main pipe easily, which makes it act as under a higher momentum ratio without changing the flow rate.

Since many different types of T-junctions are used in nuclear power plants the temperature fluctuation in the mixing tee, which causes high cycle thermal fatigue, can be decreased more than 50% by changing simple geometries of the piping system, such as the branch pipe diameter, the distance between the bend and the branch pipe, the curvature ratio of the bend, etc. The present research is useful to assess the future design of piping systems for prolonged operation.

4. REFERENCES

[1] Faidy C., "EPRI-US NRC-OECD NEA". In Third International Conference on Fatigue of reactor Components, Seville, Spain, 2004.

[2]Igarashi M. "Study on Fluid Mixing Phenomena for Evaluation of Thermal Striping in A Mixing Tee". In 10th International Topical Meeting on Nuclear Reactor Thermal Hydraulic, NURETH-10, Seoul, Korea, 2003.

[3] Hosseini S.M. " Experimental investigation of thermal-hydraulic characteristics at a mixing tee, in".In International Heat Transfer Conference, FCV-17, Sydney, Australia, 2006.

[4] Hosseini S.M. " The three-dimensional study of flow mixing phenomenon". In International Conference Nuclear Energy for New Europe, ID: 037, Bled, Slovenia, September 2005.

[5] Hosseini S.M. " Visualization of fluid mixing phenomenon". Sixth International Congress on Advances in Nuclear Power Plants, ICAPP05, ID: 5006 (R006), Seoul, Korea, May 2005.

[6] Yuki K. " vol. 2, 2001, pp. 1573–1578". In Proceedings of the Fifth World Conference on Experimental Heat Transfer Fluid Mechanics and Thermodynamics, Japan, 2004.

[7] Yuki K. "ID: N6P082".In Proceedings of the 15th International Conference on Nuclear Thermal Hydraulic, Operation and Safety (NUTHOS-6), Nara, Japan, 2004.

[8] H.C. Kao. "Some aspects of bifurcation structure of laminar flow in curved ducts", J. Fluid Mech., pp. 519–539(1992).

[9] Carmine Golia, Bernardo Buonomo, Antonio Viviani, "Grid Free Lagrangian Blobs Vortex Method with Brinkman Layer Domain Embedding Approach for Heterogeneous Unsteady Thermo Fluid Dynamics Problems". International Journal of Engineering (IJE), Volume 3, Issue 3, 313-329, May/June 2009.